The following supplements accompany the article

Overwintering strategy of sandeel ecotypes from an energy/predation trade-off perspective

Mikael van Deurs*, Asbjørn Christensen, Christina Frisk, Henrik Mosegaard

National Institute of Aquatic Resources, Technical University of Denmark, Jægersborg Alle 1, Charlottenlund Castle, 2920 Charlottenlund, Denmark

***Email: mvd@aqua.dtu.dk**

Marine Ecology Progress Series 416:201–214, 2010

Supplement 1. Parameterization of the model

Consumption (ε: Eq. (1), *V*: Eq. (3), and *a*, *b*: Eq. (4))

Specimens of small sandeel *Ammodytes tobianus*, a close relative of lesser sandeel *A. marinus*, were caught by seine and held in a 300 l tank with a 5 cm layer of sand on the bottom. Fish were starved for at least 72 h prior to each experiment. On the day of the experiment, fish (ranging from 10 to 13 cm in total length) were fed a number of meals consisting of thawed *Artemia salina* over a period of 1.5 h to ensure that the fish had reached satiation. This was necessary, since it turned out that the oesophagus constituted a bottleneck, which expressed itself as a reduction in willingness to take food after each meal. The time half way through this feeding period was defined as the time zero of the experiment. After feeding the fish to satiation, 8 fish were removed every 3 to 4 h for the subsequent 48 h and killed by a blow to the head. All sampled fish were cut open and the stomach was removed and weighed (wet weight, WW) and the total fish length was measured. This experimental procedure was carried out at 5, 10 and 17°C. Fish were acclimatized to the temperature for at least 3 wk prior to each temperature experiment.

At the beginning of the experiment (just after feeding to satiation), the 2 fullest stomachs from each half-centimetre group (fish of length 10 to 13 cm) were selected, and the weights of these were plotted against total fish length. The relationship was best described with a linear regression model of the form:

Maximum stomach content (g, WW) = 0.17 × total fish length (cm) – 1.28 ($R^2 = 0.74$).

Relative stomach fullness was calculated by dividing the weight of the stomach content with the length-specific maximum stomach content, as derived from the above linear relationship. A multiple linear regression model of the form: ln(relative stomach fullness) = time since feeding (h) × temperature (ºC) was fitted to the data (estimated coefficients were highly significant, $p > 0.001$). From this fit, we derived coefficients *a* and *b* for Eq. (4): $a = -2.7 \times 10^{-2}$ and $b = -3.6 \times 10^{-3}$.

During a previous study (authors' unpubl. data) more than 1000 sandeel stomachs from various locations in the North Sea were analysed, and the stomach content was found to consist predominately of copepods (at a few locations Larvacea were the dominant prey items). Based on this observation, a homogenous diet consisting of adult copepods was assumed in the model. Comita et al. (1966) reported that the

caloric content of adult *Calanus finmarchicus* ranged from 21 to 35.2 kJ g^{-1} of ash-free dry weight (DW). Using the midpoint of this range, 28.35 kJ g^{-1}, a WW:DW ratio of 5 (Yamaguchi & Ikeda 2000) and a weight of 500 µg (WW) for an adult copepod (Gentleman et al. 2008), the energy content of 1 prey item was calculated to be 33.5×10^{-4} kJ. Consequently, assuming that 30% of the energy of ingested food is lost to excretion, egestion and specific dynamic action (SDA) (e.g. Ciannelli et al. 1998), ε in Eq. (1) was set to 23.5×10^{-4} kJ.

Using the above derived model for maximum stomach content and a weight of 500 µg for an adult copepod, stomach capacity V in Eq. (3), for a 13 cm sandeel, was estimated to be 1860.

Energetic cost (R_A: Eq. (7) and c, d: Eq. (8))

Specimens of small sandeel were caught by seine and held in a 1500 l circular holding tank with fully oxygenated and recirculated seawater. A tube was placed in the centre of the tank. Fish in the tank emerged from the sand when light came on in the morning and swam unidirectionally as a school around the tube during all active hours of the day, until they once again buried into the sediment in the afternoon. Swimming speed was frequently measured at various times of the day at 5 and 10°C. The observed swimming velocity was assumed to resemble routine or preferred swimming velocity during foraging. With the exception of the late afternoon, just before burying, the fish swam at a velocity of ~1.5 body lengths per second, and there was no significant temperature effect.

In order to measure the energetic cost of routine swimming velocity, fish were swum, 10 at a time, in a circular respirometer, at 10ºC and without sand. Water in the circular swimming lane (height: 9 cm; width: 7.5 cm; average diameter: 32.5 cm) was pumped around to create a current within the respirometer. The water velocity was carefully measured (flowmeter from Höntzsch) at 9 different positions in each of 14 equally spaced cross sections of the swimming lane, to account for the velocity gradient. Fish maintained their position in the respirometer, except when they occasionally stopped swimming momentarily and drifted down-current to a new position. The flow velocity was therefore assumed to approximate the swimming velocity of the individual fish. The pump generating the water current was adjusted so that the fish approached the routine swimming velocity (±0.1 body lengths per second) measured in the holding tanks. The experiment was replicated 4 times at 10ºC, each time using 10 new fish that were starved for at least 48 h prior to each experiment. The measuring procedure and energy cost calculations were adopted from Behrens & Steffensen (2007), except this time the measuring period lasted 24 h and consisted of 20 min of flushing and 30 min of continuous measuring.

The energetic cost explicitly related to swimming was derived by subtracting the standard metabolic cost for buried sandeels at 10ºC from the energetic cost measured for swimming fish at the same temperature. This resulted in $R_A = 33.9 \times 10^{-4}$ kJ g^{-1} h^{-1} (the average of the experimentally measured values). We made the assumption that the energetic cost of swimming at routine velocity was independent of temperature (as long as velocity is independent of temperature) as reported by, for example, William & Beamish (1990).

The fitted coefficients c and d in Eq. (8) (standard metabolic cost for 1 g of buried sandeel as a function of temperature) were provided by M. van Deurs (pers. obs.): $c = 0.08$ and $d = 0.25$.

LITERATURE CITED

Behrens JW, Steffensen JF (2007) The effect of hypoxia on behavioural and physiological aspects of lesser sandeel, *Ammodytes tobianus* (Linnaeus, 1785). Mar Biol 150:1365–1377

Ciannelli L, Brodeur RD, Buckley TW (1998) Development and application of a bioenergetics model for juvenile walleye pollock. J Fish Biol 52:879–898

Comita GW, Marshall SM, Orr AP (1966) On the biology of *Calanus finmarchicus*. XIII. Seasonal change in weight, calorific value and organic matter. J Mar Biol Assoc UK 46:1–17

Gentleman WC, Neuheimer AB, Campbell RG (2008) Modelling copepod development: current limitations and a new realistic approach. ICES J Mar Sci 65:399–413

William F, Beamish H (1990) Swimming metabolism and temperature in juvenile walleye, *Stizostedion vitreum vitreum*. Environ Biol Fishes 27:309–314

Yamaguchi A, Ikeda T (2000) Vertical distribution, life cycle, and developmental characteristics of the mesopelagic calanoid copepod *Gaidius variabilis* (Aetideidae) in the Oyashio region, western North Pacific Ocean. Mar Biol 137:99–109

Supplement 2. Analytic solution and properties of the model

By imposing certain simplifications on the model, it is possible to solve it conceptually and analytically, which aids understanding of the patterns in the simulations. For example, it helps to identify which features and properties of the results are generic for the ecotype described by the model, and which ones are associated with the particular parameterization for the North Sea sandeel, and whether other types of results are possible for this ecotype or not.

The key approximation is averaging intake and consumption over the innermost time scale, i.e. the intraday cycle, which covers the day–night cycle and the detailed stomach evacuation dynamics. By doing this, the daily bioenergetic budget becomes dependent on the external conditions, and the state variables (e.g. instantaneous stomach fullness) associated with stomach evacuation dynamics become hidden and replaced by the average expected bioenergetic response to external conditions. In this approximation, the energy assimilation rate γ (if foraging) is:

$$\gamma(r,T) = S(r,T) - m_A\left(\frac{1}{r},T\right) \quad \text{(S1a)}$$

$$\gamma(t) = S(r(t),T(t)) - m_A\left(\frac{1}{r(t)},T(t)\right) \quad \text{(S1b)}$$

$$r(t) = \frac{v_{swim} f(t)\tau(t)}{n_o(T)} \quad \text{(S1c)}$$

where S is the functional response-modulated uptake function effectively associated with this bioenergetic model, and m_A is the cost of movement per time in relation to foraging (and temperature T). The key variable is $r = v_{swim} f\tau / n_0$, which is the potential food intake rate (the average total number of encountered prey) divided by the food intake index n_0 (which can be thought of as the cost of resting metabolism recalculated to number of prey per day), so that $r > 1$ means the fish is in a consumption-limited regime, whereas $r < 1$ means the fish is in a feeding rate-limited regime. Conversely, the ratio $1/r$ is a proxy for the activity level of the fish (if still foraging), and when $1/r >> 1$, the fish is expected to be active with a high v_{swim} for all of the daylight window τ, saturating m_A expenses, whereas $1/r < 1$ reduces m_A. Eq. (S1b) shows how the time-dependent function $\gamma(t)$ is constructed, and when and how much the actual forcing functions affect assimilation. The function $\gamma(t)$ will be a sinusoidal-like function with maximum in the summer time (in the Northern hemisphere). The function $\gamma(t)$ will have a trough in the winter time, where $\gamma(t)$ may become negative, in which case there is no energetic incentive for feeding in this period.

When averaging over the daily time scale, we can also apply an integral formulation of the energy budget, which simplifies the analysis. If the yearly active period is $[t_0; t_1]$ we obtain the total yearly energy surplus:

$$F(t_0, t_1) = \int_{t_0}^{t_1} \gamma(t) dt - M_0 \tag{S2}$$

where M_0 is the yearly total resting metabolic cost. The energy surplus F is invested in reproduction and contributes to the net lifetime reproduction. As shown in the introduction, the question about optimal overwintering strategy is now reduced to a relative simple optimization problem of the function:

$$R(t_0, t_1) = \omega \frac{FP}{1-P} \tag{S3}$$

where ω aggregates survival to adulthood and adult competition (food/habitat) effects, and P is the probability of surviving 1 yr with the given foraging strategy. Straightforward optimization ($\partial R = 0$) of Eq. (S3) gives the result:

$$\begin{cases} \gamma(t_0) = \gamma(t_1) \\ \phi(t_0) = \alpha(t_0) \end{cases} \tag{S4}$$

where:

$$\begin{cases} \phi(t_0) = \dfrac{\gamma(t_0)}{F(t_0, t_1(t_0))} \\ \alpha(t_0) = \dfrac{\Delta Z}{1 - P(t_0, t_1(t_0))} \end{cases} \tag{S5}$$

Eq. (S4) is a neat result: it tells us that the active period is $[t_0; t_1]$ is bounded by time points with the same assimilation potential γ, so if we know the starting point t_0, from a diagram of $\gamma(t)$, we can also find the ending point of the active period, indicated by $t_1 = t_1(t_0)$ in the following equation. The second equation is also neat: it tells exactly how the optimal trade-off is determined between feeding-related aspects (φ) and

mortality-related aspects (α). A little further algebra (following the second derivative of R) gives the condition for a maximum as:

$$\frac{\partial \phi}{\partial t_0} > \frac{\partial \alpha}{\partial t_0} \tag{S6}$$

at the maximum of R. This constitutes the basic analysis of the bioenergetic model.

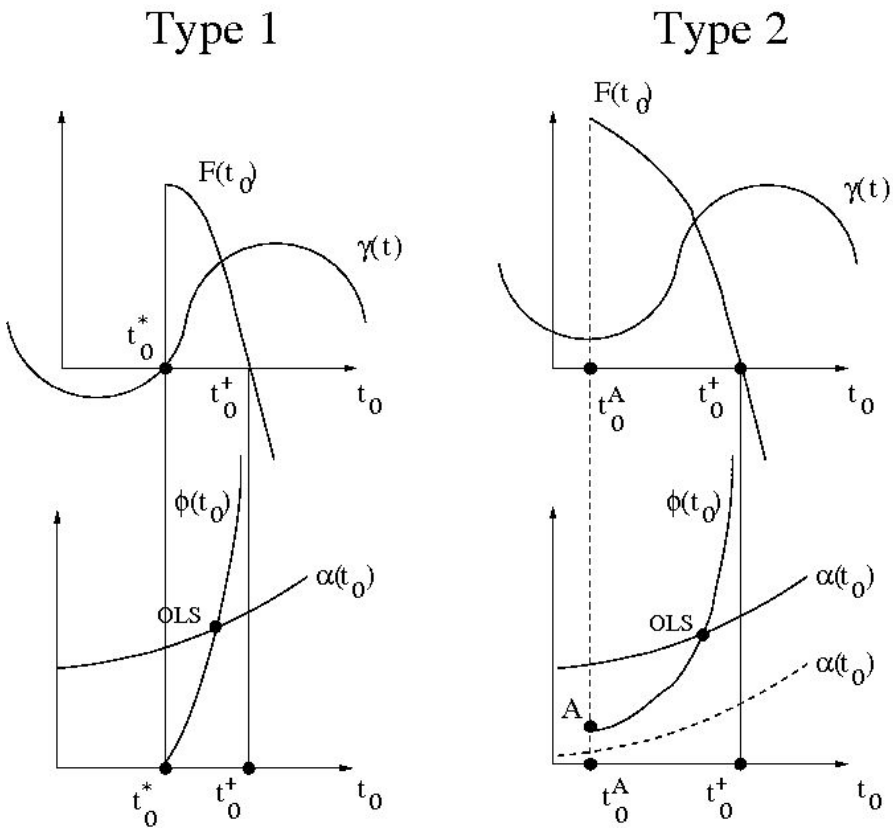

Fig. S1 Graphical illustration and interpretation of solving Eq. (S4) for the optimal overwintering strategy. The abscissa t_0 shows the starting point of the active period. The point OLS indicates the optimal life strategy solution

Fig. S1 illustrates the solution of Eq. (S4). The analysis splits into 2, depending on whether the assimilation potential $\gamma(t)$ is positive (right column) or negative (left column) at some time in the winter period. The upper row shows how the feeding-related function $\varphi(t)$ is constructed in both cases. If the active period starts very late (large t_0) the function F becomes negative: the fish is simply not able to cover the resting metabolic costs. When t_0 is moved back (i.e. longer feeding period), F increases. At a certain point—the 'break-even point' (t_0^+), $F = 0$ and the fish is just able to cover basic metabolic costs, but without energy for reproduction. Moving t_0 further back makes F positive. The lower row shows $\varphi(t)$ constructed from γ and F in the upper row for both types. The major difference between Type 1 and 2 is that the root of γ leads to a root for φ for Type 1, whereas φ for Type 2 ends at a positive

value at point A (lower left, where the active period covers all year). Simple arguments show that $\alpha(t_0)$ is a monotonously increasing function of t_0, as sketched in the figure. This implies that Type 1 always has a single optimal overwintering strategy, for any mortality and feeding level. For Type 2 there is only an overwintering period if $\alpha(t)$ crosses $\varphi(t)$ (solid curve α). If $\alpha(t)$ creeps below $\varphi(t)$ (dashed curve α), no overwintering period is predicted at all. This happens, if the arena mortality is very low (i.e. very low ΔZ). The transition happens, when $\alpha(t)$ crosses the point A in the lower right figure.

When the analysis above gives a true maximum of Eq. (S3), $R(t_0, t_1)$, one further condition must be assured, namely that $R(t_0, t_1) > 1$; in that case population density effects will downregulate ω by increasing the population size, so that eventually $R(t_0, t_1) \sim 1$, and the population is stable (or quasistable). ω is a decreasing function of the population density; this means that it has an upper bound ω_0. Therefore, if a (quasi)stable population should be attainable by self regulation, the following condition must also be fulfilled:

$$\omega_0 > \frac{1-P}{FP} = \eta(t_0) \qquad \text{(S7)}$$

at the maximum of R; otherwise the population will eventually become extinct. This will be the case in Fig. S1 (lower left) with sufficiently high fishing pressure (large α). Thus Eq. (S7) introduces the extinction function $\eta(t_0)$, where $t_1 = t_1(t_0)$ has been applied again. The biological interpretation of Eq. (S7) is also clear: if the surplus on the bioenergetic budget is low (F small or negative) or if the yearly survival chance is low (P low), population density effects are not able to reinstate the population level. The resilience capacity ω_0 of the ecotype is given by the biology of the species and the ecosystem hosting the ecotype.

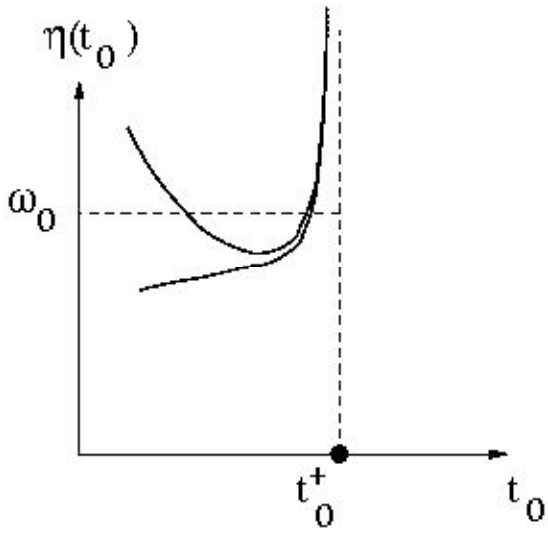

Fig. S2 The generic form of the extinction function $\eta(t_0)$, which can take either of the 2 curve forms indicated

Based on Fig. S1, the generic form of the extinction function $\eta(t_0)$ can be sketched, as shown in Fig. S2 above. The sketch applies to both Types 1 and 2 introduced in Fig. S1. Generally, $\eta(t_0)$ diverges as t_0 approaches the bioenergetic 'break even point' t_0^+ (because F approaches zero), where feeding just balances basic metabolic costs; this means Eq. (S7) always lowers the actual 'break even point'. Depending on the actual curve shape in Fig. S2 and the actual resilience capacity ω_0 of the ecotype, Eq. (S7) may also make very long active periods unsustainable on the long term (even though they correspond to a maximum of R).

Finally, it is of interest to understand the potential impact of changed fishing mortality. Change in fishing mortality will influence the predicted optimal overwintering strategy by shifting $\alpha(t)$ up or down in Fig. S1. Simple differentiation and Fig. S1 show that

$$sign(\frac{\partial t}{\partial \Delta Z}) = sign(\frac{\partial \alpha}{\partial \Delta Z}) = sign(1 - P - \Delta Z(t_0 - t_1)P) \qquad \text{(S8)}$$

In the biologically relevant parameter regime we always find that $\partial\alpha/\partial\Delta Z > 0$, so that isolated increased fishing mortality (increasing ΔZ) always reduces the active foraging period by Eq. (S8) (and may further cause stock collapse, if Eq. S7 becomes violated). In fishery management contexts, Eq. (S7) can also be used as a device to estimate the proximity to stock collapse for this ecotype.